

# DIRECTIVITY AND SENSITIVITY OF HIGH FREQUENCY CARRIER TYPE THIN-FILM MAGNETIC FIELD SENSOR

M. Yamaguchi<sup>a</sup>, M. Takezawa<sup>a</sup>, H. Ohdaira<sup>b</sup>, K. I. Arai<sup>a</sup>, and A. Haga<sup>b</sup>

<sup>a</sup>*Research Institute of Electrical Communication, Tohoku University, 2-1-1 Katahira, Aoba-ku, Sendai 980-8577, Japan*

<sup>b</sup>*Dept. of Electrical Engineering, Tohoku Gakuin University, 13-1 Chuo 1-chome, tagajo 985-8537, Japan*

## Abstract

We discuss the directivity and sensitivity of high frequency carrier type thin-film magnetic sensor (or so-called MI sensor.) The inductance of the sensor changes as a function of the angle,  $\theta$ , between the applied magnetic field,  $H_{dc}$ , direction and the length direction of the sensor. The relation between the inductance and the angle is  $\cos^3\theta$  because the inductance varies as  $H_{dc}^3$ . The effective magnetic field inside the magnetic thin-film is proportional to  $H_{dc} \cos\theta$  because of the rectangular shape. Moreover, the high sensitivity of  $2 \times 10^{-4}$  Oe has been demonstrated provided a 140 MHz carrier current and lock-in amplifier detection.

*Keywords* : Directivity; Sensitivity, Demagnetizing factor, Effective field, Inductance

## 1. Introduction

Thin-film type miniature sensors are advantageous over bulk sensors[1] on the space resolution, mass-production capability and integration capability with semiconductor circuit, etc. Therefore high frequency carrier type thin-film magnetic sensors using impedance change of soft magnetic thin-films have been studied because the sensor have high sensitivity, coilless configuration, etc. It has been proposed that the high frequency carrier type sensor is applicable in the three dimensional position sensor of a small magnetic marker[2]. The high sensitivity and simple directivity are required to detect the position of the marker which has a very weak and localized magnetic field. The gain of 2.0V/Oe has already been demonstrated by us for bridge connected sensor[3] with CMOS-IC detection circuit whose carrier frequency was 15 MHz and dc bias field along hard axis of magnetization of 4.5 Oe. The purpose of this paper is to examine the directivity and sensitivity of the sensor

considering the noise.

## 2. Experimental Procedures

Fig.1 shows the schematic view of the fabricated sensor. The element is a rectangular strip of an amorphous  $\text{Co}_{0.84.85}\text{Nb}_{12}\text{Zr}_{3.15}$  thin-film. 3 or 6  $\mu\text{m}$  thick CoNbZr films were rf-sputter deposited onto soda glass substrates and then patterned into 100  $\mu\text{m}$  wide and 5 mm long rectangle. The sensor element was annealed during 2 hours at 400 °C in a 60 rpm rotating magnetic field of 500 Oe, followed by 1 hour at 400 °C in a static magnetic field of 500 Oe in order to induce uniaxial magnetic anisotropy. The anisotropy field,  $H_k$ , of the sensor was 5 ~ 6 Oe. Sensor's easy axis of magnetization is along the width direction.

Applying high frequency current of 10 MHz to the length direction of the element which is 6  $\mu\text{m}$  thick, we measured the impedance of the elements using a network analyzer (HP8752A). The element was submitted to an external dc field,  $H_{dc}$ , in order to determine the directivity of the sensor elements. Let the angle between the applied magnetic field direction and the length direction of the sensor be  $\theta$  as shown in Fig. 2. The external dc field was applied using a helmholtz coil.

Amplitude and phase of the output voltage of the sensor element were detected with a high frequency lock-in amplifier (SRS-SR844) at 140 MHz, when the sensor was supplied a small dc magnetic field change of  $10^{-3} \sim 10^{-4}$  Oe to clarify the sensitivity of the sensor. In this case, the thickness of the sensor was 3  $\mu\text{m}$ . In order to obtain a high sensitivity, a constant dc bias field of 5.5 Oe was applied. The sensor was set in a magnetic shield case and we used chemical batteries to supply a constant current to solenoid coils so the external noise could be decreased.

## 3. Results and Discussion

Fig. 3 shows the dependence of the impedance,  $Z$ , resistance,  $R$ , and inductance,  $L$ , on the external dc field,  $H_{dc}$ , at carrier frequency of 10 MHz when  $\theta$  changed from 0 to 90 degree on the film plane.  $Z$ ,  $R$  and  $L$  at 0 deg. increased with the increase of the dc magnetic field, and were maximum when  $H_{dc}$  nearly equals  $H_k$  of the magnetic films. Maximum values of  $Z$ ,  $R$  and  $L$  were 13.6  $\Omega$ , 12.8  $\Omega$  and 69.6 nH respectively. The magnetic field at which  $Z$  reached a maximum, increased with the increase of  $\theta$  from 0 to 80 deg. And  $Z$ ,  $R$  and  $L$  were roughly constant at 90 deg.

Fig. 4 shows the dependence of  $Z$ ,  $R$  and  $L$  on the  $H_{dc}$  when the sensor was rotated perpendicularly to the film plane. The  $\theta$  was 0, 30, 60 and 90 deg. Results are quantitatively identical to the case of the in-plane rotation as shown in Fig. 3. The reason for the results is that the length of the sensor is much longer than the thickness and width.

Values of inductance, resistance and impedance at  $H_{dc} = 5$  Oe were obtained from Fig. 4. The data is shown as a function of the angle,  $\theta$ , in Fig. 5.  $Z_\theta$ ,  $R_\theta$  and  $L_\theta$  are the normalized impedance, resistance and inductance as follows.

$$Z_\theta = (Z - Z_{90}) / (Z_0 - Z_{90}) \quad (1)$$

$$R_\theta = (R - R_{90}) / (R_0 - R_{90}) \quad (2)$$

$$L_\theta = (L - L_{90}) / (L_0 - L_{90}) \quad (3)$$

where  $Z_{90}$ ,  $R_{90}$  and  $L_{90}$  are impedance, resistance and inductance at  $\theta = 90$  deg. and  $Z_0$ ,  $R_0$  and  $L_0$  are  $Z$ ,  $R$  and  $L$  at  $\theta = 0$ . In Fig. 5,  $L_\theta$  was proportional to  $\cos^2 \theta$  in the case of  $\theta = 0 \sim 30$  deg. and was proportional to  $\cos^3 \theta$  at  $\theta = 50 \sim 90$  deg. This relation holds for both rotation in the film plane and rotation perpendicularly to the film plane.

Magnetic field dependence of inductance when  $\theta = 0$  deg. is shown in a log-to-log scale in Fig. 6. This figure is the re-write of the corresponding data as obtained in Fig. 3(a) and Fig. 4(a). Here the inductance is normalized form as follows.

$$L_H = (L - L_0) / (L_5 - L_0) \quad (4)$$

where  $L_0$  is the inductance at  $H_{dc} = 0$  and  $L_5$  is the inductance at  $H_{dc} = 5$  Oe. The inductance was minimum at  $H_{dc} = 0$  and was maximum at  $H_{dc} = 5$  Oe. Therefore the range of  $L_H$  was between zero and unity.  $L_H$  varied as  $L_H = 0.008 H_{dc}^3$  when  $H_{dc} = 1.5 \sim 5$  Oe. Let define the effective field intensity in the sensor element as  $H_{in}$ . The direction of  $H_{in}$  was always along the length direction. If  $\theta = 0$ ,  $H_{in}$  equals  $H_{dc}$  because the demagnetizing factor,  $N_l = 0.000048$ , along the length direction of the sensor element was much smaller than the demagnetizing factor along another two axes,  $N_w = 0.059986$ ,  $N_t = 0.939966$ . Therefore  $L_H$  is given by the following expression.

$$L_H = 0.008 H_{dc}^3 = 0.008 H_{in}^3 \quad (5)$$

If  $\theta$  was deviated from zero, magnetic field intensity along the length direction of the sensor element was  $H_{dc} \cos \theta$ . But the effective field intensity  $H_{in}$  did not always equal  $H_{dc} \cos \theta$  because the direction of magnetization of a rectangular magnetic body is deviated from the length direction at the edge as simulated in Fig. 7 by FEM. It is also seen in Fig. 7 that the direction of magnetization at the film center remained almost paral-

lel to the length direction except  $\theta = 90$  deg. portion. This means that it is a reasonable approximation that the direction of the effective field  $H_{in}$  is along the length direction. Assuming that the value of inductance in Fig. 5 varies as a function of the effective field  $H_{in}$ , we can graphically estimate  $H_{in}$  as a function of  $\theta$  as follows: (i) For a given angle  $\theta_x$  in Fig. 5, find out a corresponding normalized inductance  $L_\theta = L_x$ . (ii) Calculate the inductance  $L = L_x^*$  using eq.(3). (iii) In Fig. 4(a) on the  $\theta = 0$  deg. curve, find out a magnetic field intensity  $H_x$  corresponding to  $L_x^*$ . Then  $H_{in}=H_x$ . (iv) Repeating (i)-(iii) for different angles, we obtain Fig. 8. The  $H_{in}$  varies as  $\cos\theta$  for both in-plane rotation and perpendicular to plane rotation as shown in Fig. 8. Because of the results,  $H_{in}$  agrees with the  $H_{dc}\cos\theta$ . Substituting this relation into eq. (5), we obtain  $L_\theta \propto \cos^3\theta$ , which well explains the physical meaning of Fig. 6. This simple relation of  $H_{in} = H_{dc}\cos\theta$  is very useful when determining the direction of the field.

Figure 9 shows the direction of the field sensor output when dc field step  $\Delta H_{dc}$  of  $2 \times 10^{-4}$  Oe was applied. The corresponding output voltage change,  $\Delta V$ , was about  $15 \mu V$ . The fluctuation of the background noise were about  $10 \sim 15 \mu V$ . The field resolution was thus estimated to be  $2 \times 10^{-4}$  Oe.

#### 4. Conclusion

The  $\cos^3\theta$  relation between the inductance of the high frequency carrier type thin-film magnetic sensor and the applied magnetic field direction was obtained. If the inductance was proportional to the external magnetic field, simple relation of  $H_{in} = H_{dc}\cos\theta$  could be achieved. The sensor was estimated to exhibit a field resolution of  $2 \times 10^{-4}$  Oe.

#### Acknowledgements

We would like to thank Tokin Co., Ltd. for measurement by using the magnetic shield case. This study was partially supported by the Program for Promotion of Fundamental Studies in Health Sciences of the Organization for Drug ADR Relief, R & D Promotion and Product Review of Japan.

## References

- [1] K. Bushida, K. Mohri, Highly sensitive and quick-response colpitts-oscillator-type current sensor using an amorphous magnetic wire MI element, *J. Magn. Soc. Jpn.*, 20 (1996) 629 – 632.
- [2] T. Uchiyama, K. Mohri, M. Shinkai, A. Ohshima, H. Honda, T. Kobayashi, T. Wakabayashi and J. Yoshida, Position sensing of magnetite gel using MI sensor for brain tumor detection, *IEEE Trans. Magn.*, 33 (1997) 4266 – 4268.
- [3] M. Takezawa, H. Kikuchi, K. Suezawa, K. Ishiyama, M. Yamaguchi and K. I. Arai, High frequency carrier type bridge-connected magnetic field sensor, *IEEE Trans. Magn.*, 34 (1998 in press).
- [4] A. Haga, M. Yamaguchi and K. I. Arai, Analysis on Magnetization of Magnetic Sheets, *IEEJ Magn. Soc. Jpn.*, (1993) MAG-93-140

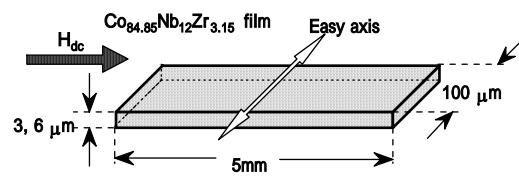


Fig. 1. Schematic view of the high frequency carrier type thin-film sensor.

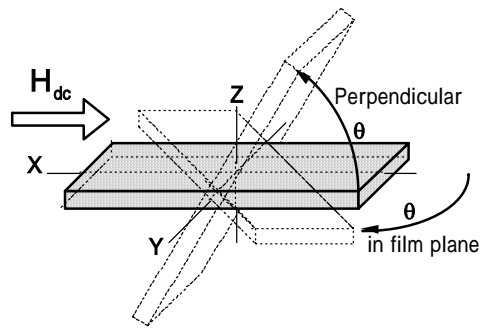
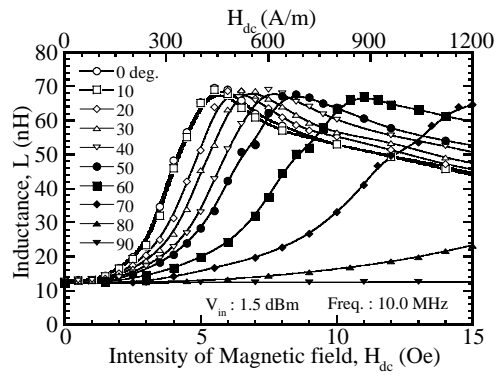
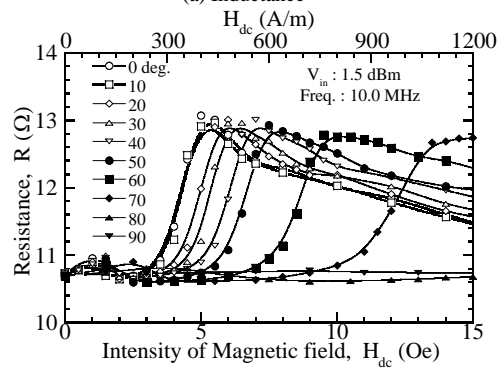


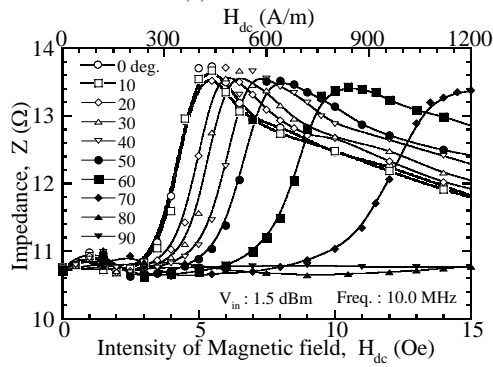
Fig. 2. External magnetic field direction.



(a) Inductance



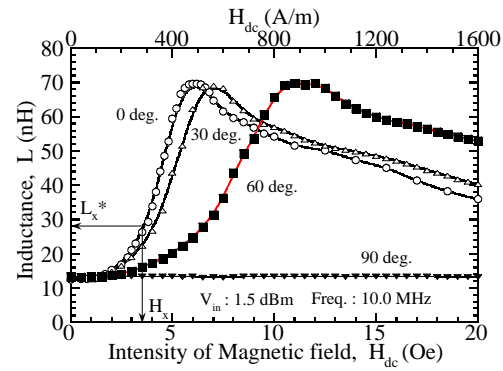
(b) Resistance



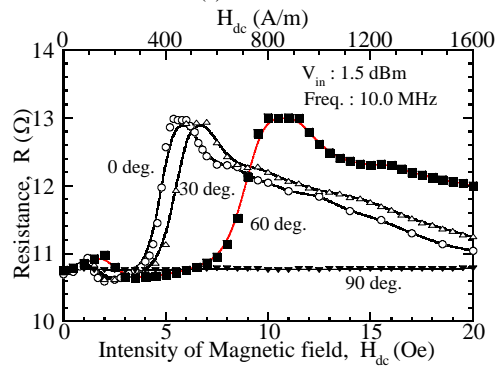
(c) Impedance

Fig. 3. Dependence of the inductance, resistance and impedance on the external dc magnetic field when the sensor was rotated on the film plane.

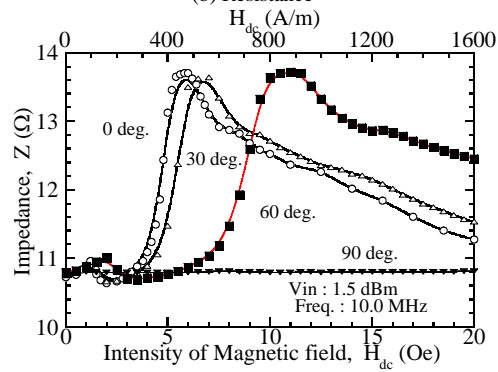




(a) Inductance



(b) Resistance



(c) Impedance

Fig. 4. Dependence of the inductance, resistance and impedance on the external dc magnetic field when the sensor was perpendicularly rotated to the film plane.

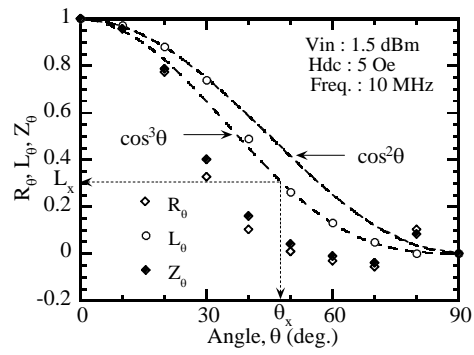


Fig. 5. Dependence of  $R_\theta$ ,  $L_\theta$  and  $Z_\theta$  on the  $\theta$  at  $H_{dc} = 5$  Oe.

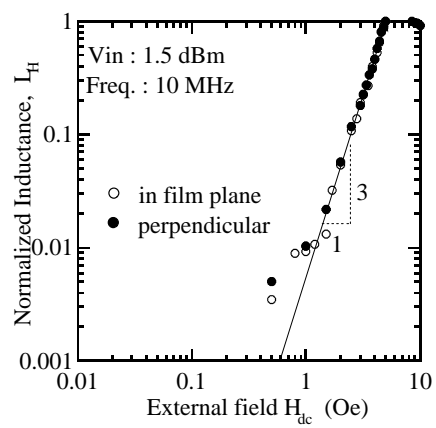


Fig. 6. Dependence of L on the external field.

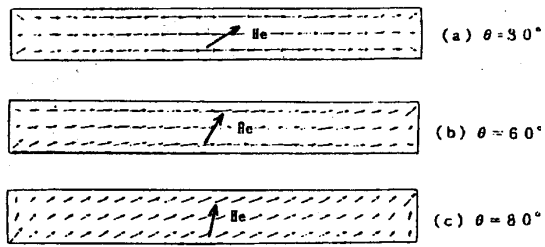


Fig. 7. Magnetization inside rectangular magnetic material[4].

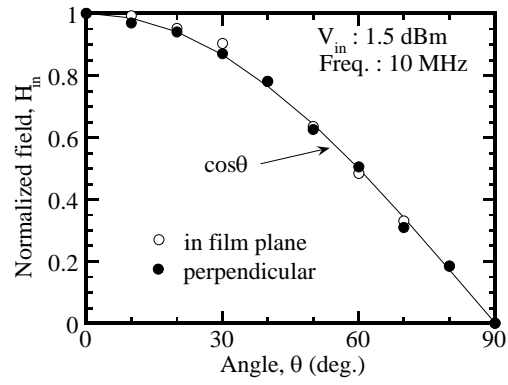


Fig. 8. Dependence of the effective field inside magnetic thin-film on the angle.

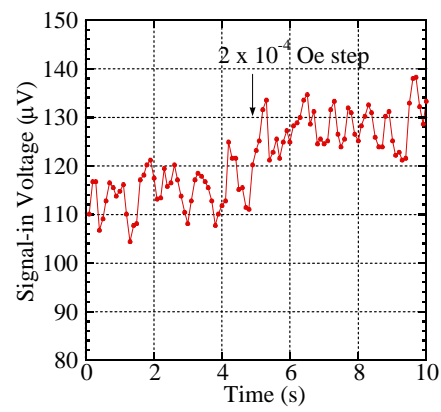


Fig. 9. Amplitude of the sensor output at the small dc field change,  $\Delta H_{dc}$ , of  $2 \times 10^{-4}$  Oe.